



**Ester-Substituted Cyclometallated Rhodium and Iridium
Coordination Assemblies with pi-Bonded Dioxolene ligand :
Synthesis, Structures and Luminescent Properties**

Journal:	<i>RSC Advances</i>
Manuscript ID:	RA-ART-02-2014-001185.R1
Article Type:	Paper
Date Submitted by the Author:	18-Apr-2014
Complete List of Authors:	Amouri, Hani Haniel; UPMC, Chemistry Barbieri, Andrea; Consiglio Nazionale delle Ricerche (CNR), Istituto per la Sintesi Organica e la Fotoreattività (ISOF) Gullo, Maria; Consiglio Nazionale delle Ricerche (CNR), Istituto per la Sintesi Organica e la Fotoreattività (ISOF) Rager, Marie; ENSCP, Damas, Aurelie; UPMC, Chemsitry Sesolis, Hugo; UPMC, Chemsitry Chamoreau, Lise-Marie; Universite Pierre et Marie Curie, Institut Parisien de Chimie Moléculaire

Cite this: DOI: 10.1039/c0xx00000x

www.rsc.org/xxxxxx

ARTICLE TYPE

Ester-Substituted Cyclometallated Rhodium and Iridium Coordination Assemblies with π -Bonded Dioxolene ligand : Synthesis, Structures and Luminescent Properties

Aurelie Damas,^{†1,2} Hugo Sesolis,^{†1,2} Marie Noelle Rager,[§] Lise Marie Chamoreau,^{†1,2} Maria Pia Gullo,[‡]
5 Andrea Barbieri,^{*‡} and Hani Amouri^{*†1,2}

Received (in XXX, XXX) Xth XXXXXXXXX 20XX, Accepted Xth XXXXXXXXX 20XX

DOI: 10.1039/b000000x

A series of functionalized cyclometallated rhodium and iridium coordination assemblies 2-7 displaying a π -bonded dioxolene ligand is described. The X-ray molecular structures of two of the above compounds
10 showed the formation of 1D supramolecular chain mediated by π - π interactions among individual units. The luminescent properties of these compounds are presented and discussed. These results show that the stacking interactions are retained also in solution and emission from excited dimeric species is observed.

Introduction

Coordination compounds of the redox active 1,2-dioxolene
15 chelating ligands have been well investigated since the mid 70s by the group of C. G. Pierpont,¹ and later by the groups of Lever² and Ward,³ due to their intriguing electrochemical and photophysical properties.⁴ In these complexes, a strong degree of orbital mixing between metal $d(\pi)$ and ligand $p(\pi)$ frontier
20 orbitals renders conventional assignment of the oxidation state, based on localized charges, difficult. The different redox states of dioxolene ligands generally have distinct spectroscopic characteristics, and their metal complexes show intense charge transfer (CT) bands appearing in different regions of the
25 spectrum as the oxidation state changes.^{4a} For instance, ruthenium complexes show a strong near-infrared (NIR) absorption when the ligand is in the semiquinone form [Ru(II)/sq⁻], due to a Ru($d\pi$) \rightarrow sq(π^*) metal-to-ligand charge transfer (MLCT) band which disappears in the fully reduced
30 catecholate form [Ru(II)/cat²⁻] or is moved to higher energy in the visible region in the oxidized [Ru(II)/q] state.⁵

Due to their electronic structures, such complexes have found numerous applications e.g. they have been proposed as redox-switchable electrochromic dyes, for modulation of optical signals
35 and smart windows,⁶ as magnetic materials,⁷ as NIR sensitizers⁸ and anchors⁹ to semiconductor surfaces in organic photovoltaic cells, and in application related to solar energy conversion,^{4b} as components of modified electrodes,¹⁰ and as extended assemblies for electron and energy transfer incorporating both organic and
40 coordination compounds.¹¹ On the other hand, such metal dioxolene complexes do not exhibit luminescent properties, which preclude a number of new applications. In fact, the redox-active substituents introduce accessible low-energy electronic transitions, which lead to quenching of the metal center
45 luminescence by an electron transfer mechanism.²⁰

The research in this area has been focused mainly on d^6 transition metal complexes,¹² such as ruthenium,^{3,13} osmium,¹⁴ chromium,¹⁵ manganese,¹⁶ and rhenium,¹⁷ and on the properties of the
50 electronic ground states of such compounds, while there have been fewer reports on the properties of rhodium,¹⁸ iridium,¹⁹ and platinum²⁰ complexes with dioxolene ligands. To our knowledge only one cyclometallated iridium complex with semiquinone ligand was reported by *Thompson et al.*

We previously shown that organometallic moieties and in particular "Cp*M, M = Ru, Rh and Ir can stabilize reactive intermediates by modifying their electronic properties.²¹ Among which π -bonded quinonoid complexes of the formula [Cp*M(*o*-C₆H₄E₂)]ⁿ, where E = O, M = Ru, n = -1; M = Rh, Ir, n = 0, Cp*
55 = pentamethyl-cyclopentadienyl.²¹ The related thio-²² and seleno-quinonoid π -complexes were also prepared.²³ These π -bonded quinonoid compounds were found to be adequate OM-ligands for the preparation of a new class of luminescent supramolecular
60 assemblies.^{24-26,30} In fact the presence of Cp*M renders the π -bonded quinone ligand more donor (*i.e.* acquires more catecholate contribution) and enhances the solubility of the obtained supramolecular assembly.

More recently we discovered that the use of different Cp*M moieties in the metallo-ligands allowed us to optimize the
70 electronic properties of an octahedral [M(L-L)₂(Cp*M(*o*-C₆H₄O₂))] ²⁺ complex, giving rise to materials with panchromatic absorption with high oscillator strengths and unprecedented luminescent behavior.^{26,30} Because this complex-as-ligand approach proved to be very effective in the modulation of the
75 electronic properties of Ru(II) polypyridyl complexes, we sought the preparation of a novel class of luminescent cyclometallated metal complexes containing π -bonded dioxolene ligands. In this paper, we report on the synthesis and photophysical characterization of a series of bimetallic rhodium and iridium
80 cyclometallated complexes displaying a π -bonded *o*-benzoquinone ruthenium complex (Chart 1). The molecular

structures of two compounds were determined by single crystal X-ray diffraction study. Furthermore these compounds show strong luminescence in condensed media.

5 Results and Discussions

Synthesis of the ester-substituted cyclometallated rhodium and iridium assemblies [(mpcpy)₂M(1)] (2-3) with the π-bonded quinonoid ruthenium complex.

The binuclear coordination assemblies [(mpcpy)₂Rh(1)] (2) and [(mpcpy)₂Ir(1)] (3) were prepared in two steps, the first step involved the *in-situ* synthesis of the solvated cyclometallated metal complexes [(mpcpy)₂M(solvent)₂][OTf] with methyl-2-phenyl-4-carboxypyridine (mpcpy) from the chloro-bridged dimer [M(mpccp)₂(μ-Cl)₂ and AgOTf in acetone at room temperature. Then in a second step the π-bonded ruthenium compound [Cp*Ru(o-C₆H₄O₂)] [Cs] (1-Cs) prepared in acetone was added and the mixture was left to stir for one hour. Reaction work-up allowed the isolation of the target compounds [(mpcpy)₂Rh(1)] (2) and [(mpcpy)₂Ir(1)] (3) as dark yellow and purple microcrystalline solids respectively in almost quantitative yields.

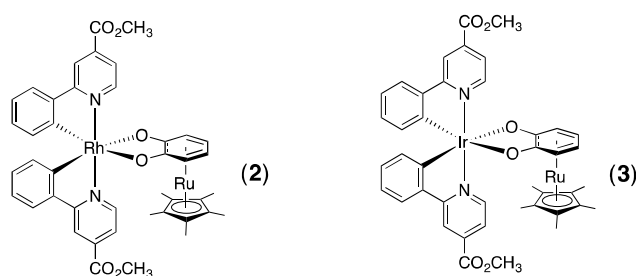


Figure 1. Schematic drawing of the ester-substituted cyclometallated coordination assemblies 2-3

These compounds were fully characterized by (¹H and ¹³C) NMR spectroscopy and elemental analysis moreover the X-ray molecular structures were determined (*vide infra*). In particular the ¹H-NMR spectrum of [(mpcpy)₂Ir(1)] (3) recorded in CD₂Cl₂ showed the expected resonance patterns for the unsymmetrical coordination assembly with 14 resonance signals assigned to the cyclometallated unit in the range of 6-10 ppm while the protons of the π-bonded catecholate gave four signals due to the lack of symmetry in the area 4.2 -5 ppm, further the two methyl groups of the esters appeared as singlet at 3.97 and 4.05 ppm while the protons of the Cp*Ru gave a singlet at 1.69 ppm. Full characterization of both compounds is given in the experimental section.

X-ray molecular structures of the ester-substituted cyclometallated rhodium and iridium complexes 2-3 and formation 1D supramolecular chains.

Convenient crystals of compounds 2 and 3 were obtained by diffusion of hexane into a dichloromethane solution of either complex. Crystals of 2 are brown and those of 3 are purple and they crystallize in the triclinic P1 and monoclinic C2/c space groups respectively. The molecular structure of 2 is shown in Figure 2. The structure of 2 shows the OO chelating mode of the organometallic ligand 1 to the Rh(ppy)₂ core through the two

oxygen centers. The Rh(III) center is coordinated to two cyclometallated mpcpy ligands with *cis* metallated carbons and *trans* nitrogen atoms as expected for this type of L₂Rh(ppy)₂ complexes, and thus describing a distorted octahedral geometry. The Rh---N and Rh---C bond distances are on average 2.027 Å and 1.980 Å and fall in the usual range as expected for L₂Rh(ppy)₂ compounds. The structure reveals that the carbocycle ring is coordinated to Cp*Ru through only four carbons in η⁴-fashion, thus the Ru1---C29-32 bond distance on average is 2.196 Å for the internal diene system while those for Ru1---C27 and Ru1---C28 distances are of 2.46 Å and 2.36 Å, respectively, indicating the absence or a weak interaction. Moreover, the C27---O1, C28---O2 and C27---C28 bond distances are of 1.294 Å, 1.289 Å and 1.460 Å respectively. The hinge angle across the C29—C32 is of 7.09° which represents a small deviation from planarity. All over the X-ray structure of 2 suggests that in the solid state a more *catecholate resonance* form can be ascribed to the π-bonded dioxolene ligand. Similar structural features were found to the related iridium congener [(mpcpy)₂Ir(1)] (3) which is presented in the SI section.

Examining the packing of complex 2 in the solid state suggested the formation of 1D supramolecular assembly composed of individual units that undergo π-π stacking between the phenyl ring of one mpcpy unit and the functionalized pyridine ring of another mpcpy ligand (3.555Å and 3.680 Å). These π-π interactions occurred in two different directions (see Figure 2b).

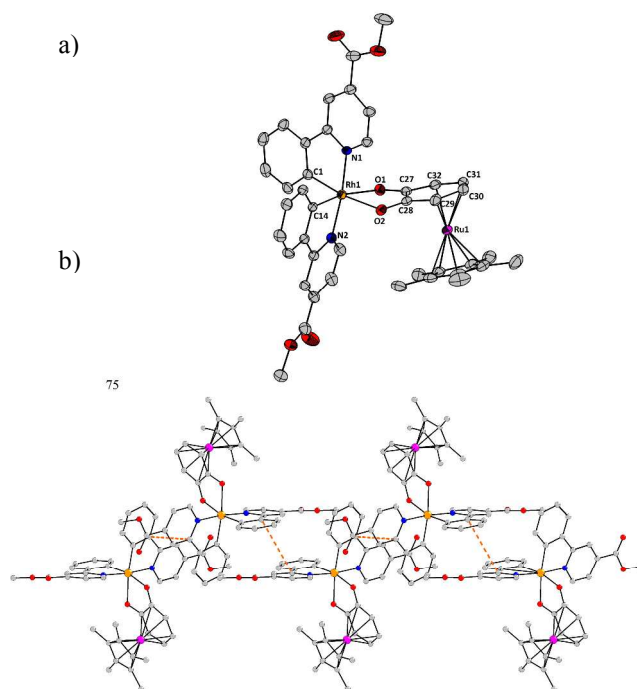


Figure 2. a) Molecular structure of [(mpcpy)₂Rh(1)] (2) with atom partial numbering system. b) Solid state packing between individual units showing π-π interactions to generate 1D supramolecular chain.

Synthesis of the ammonium and lithium acetate-substituted cyclometallated rhodium and iridium assemblies [(TBAmpcy)₂M(1)] (4-5) and [(Lipcpy)₂M(1)] (6-7)

The ester-substituted cyclometallated complexes 2-3 served as

starting materials to prepare the related acetate compounds, which were obtained as tetrabutylammonium [(TBAp_{py})₂M(**1**)] (**4-5**) and lithium [(Lipcpy)₂M(**1**)] (**6-7**) salts (Figure 3).

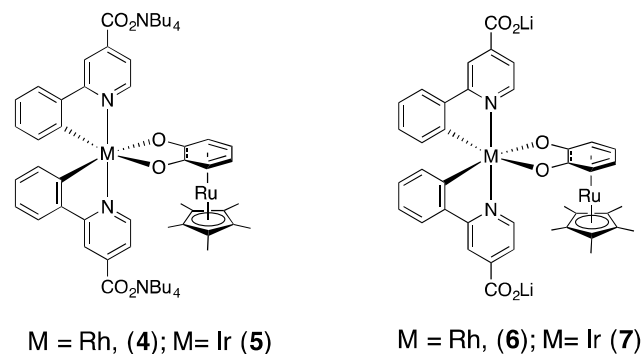


Figure 3. Schematic drawings for acetate-salts of the cyclometallated rhodium and iridium coordination assemblies **4-7**.

Complexes **4** and **5** were obtained by treatment of [(mpcpy)₂Rh(**1**)] (**2**) and [(mpcpy)₂Ir(**1**)] (**3**) with NBu₄OH in EtOH/H₂O (9:1) respectively for 6 hours at room temperature. Reaction work-up provided the acetate compounds in high yields. These assemblies were fully characterized by spectroscopic technique and elemental analysis (see experimental section). The related acetate complexes **6-7** with lithium salts were obtained by treatment of the cyclometallated complexes **2-3** with LiOH in EtOH/H₂O (9:1) but for longer period of time 18 hours. The binuclear compounds **6-7** were also obtained in high yields and fully characterized including elemental analysis. Having obtained this unique type of cyclometallated rhodium and iridium complexes with π -bonded dioxolene ligands, we investigated their photophysical properties.

Photophysical properties of the functionalized cyclometallated rhodium and iridium coordination assemblies **2-7**

The absorption spectra of complexes **2-7** recorded at rt in CH₃OH solutions are reported in Figure 4, and relevant data are collected in Table 1.

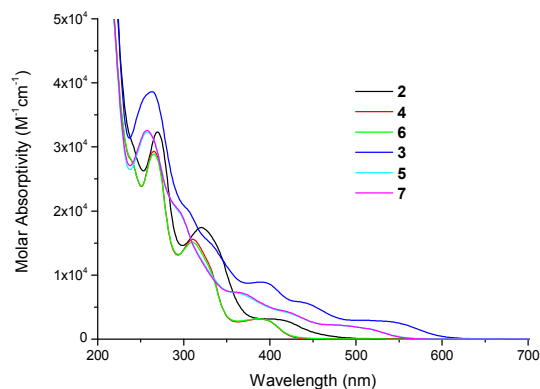


Figure 4. Absorption spectra of **2-7** in CH₃OH solution at rt.

The absorption profiles of the ester derivatives **2-3** show a similar high-energy band peaking around 260–270 nm. This originates from spin-allowed ¹ π, π^* ligand-centred (¹LC) transitions of the phenylpyridine ligands, with some likely

contribution from ³LC forbidden transitions,²⁷ enabled by the heavy-atom effect of the iridium and rhodium nuclei ($\zeta_{Rh} = 1259 \text{ cm}^{-1}$; $\zeta_{Ir} = 3909 \text{ cm}^{-1}$).²⁸ In the lower energy spectral region between 350 and 500 nm they show an envelope of low intensity absorption bands ($\epsilon < 10^4 \text{ M}^{-1} \cdot \text{cm}^{-1}$) of less straightforward attribution. For these features it seems reasonable to consider not only ¹MLCT transitions related to the iridium(III) and rhodium(III) phenylpyridyl moieties but also CT transitions from the occupied d metal orbitals to the π^* MOs of the metallated dioxolene moiety, either of σ bond to ligand charge transfer (¹SBLCT) or mixed ¹MLCT/intravalent charge-transfer (¹ILCT) character.²⁹ In fact, it has been shown that in these types of complexes, when the OM-linker with ruthenium is present, the catecholate ring significantly participates in the description of the highest occupied MOs (HOMOs).³⁰ On the other hand, the low energy virtual MOs (LUMOs) are almost completely centred on the ppy ligands.³⁰ The ionic complexes **4-7** display absorption features, independent from the type of cation, similar to those of the respective parent complexes **2-3**, but with all transitions blue-shifted. This effect is originated from the presence of the carboxylate group on the pyridine moiety of the ppy ligand.

Table 1. Absorption parameters^a

	λ_{max} , nm ($\epsilon_{\text{max}} \times 10^{-3}, \text{M}^{-1} \cdot \text{cm}^{-1}$)
2	270 (32.3), 321 (17.4), 400 (3.1)
4	265 (29.3), 311 (15.6), 388 (3.1)
6	265 (28.9), 310 (15.1), 386 (3.2)
3	263 (38.6), 302 sh (20.6), 325 sh (15.7), 390 (8.9), 431 sh (5.9), 516 (2.9)
5	257 (32.3), 290 sh (20.6), 365 (7.1), 413 sh (4.4), 476 (2.2)
7	257 (32.6), 291 sh (20.6), 360 (7.3), 414 sh (4.5), 472 (2.2)

^a In CH₃OH solution at rt. sh is shoulder

The normalized luminescence spectra obtained at 77 K in a MeOH:EtOH (1:4) mixture are reported in Figure 5, and the relevant photophysical parameters are summarized in Table 2. The rhodium derivatives **2, 4, 6** are non emissive in solutions at rt, while the iridium containing complexes **3, 5, 7** display a weak emission, $\phi = 0.5\text{-}5.2 \times 10^{-3}$ in de-aerated solution, with mono-exponential decays in the ns range (Table 2 and Figure 1 ESI). At odds with their room temperature behaviour, all complexes **2-7** were found to intensely luminesce at 77 K.

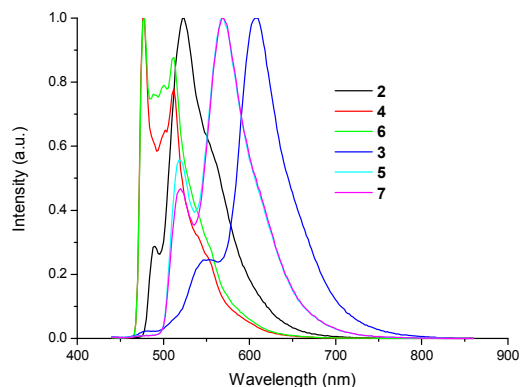


Figure 5. Emission spectra of **2-7** in MeOH:EtOH (1:4) mixture at 77 K.

The Rh derivatives **4** and **6** show a structured emission, at odds

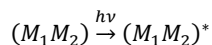
with the other investigated complexes, which display an almost featureless spectral profile. Further, the emissions from the Rh containing complexes are all blue-shifted with respect to that of the corresponding Ir derivatives **3**, **5** and **7**. The luminescence spectra of the esters **2** and **3** again differ from that of the relevant ionic complexes **4-7**, which are almost coincident in pair for instance complexes **4** and **6** for the rhodium series and **5** and **7** for the iridium congener (see Figure 6), as already observed in the case of the absorption spectra. The emission observed at low temperature for the iridium derivatives **3**, **5** and **7** is blue-shifted with respect to room temperature, a typical feature of an excited state with charge transfer (CT) nature. In fact, in solid matrix the reorganization of the solvent molecules surrounding the complex following the charge transfer event is prevented, and the excited state is destabilized by the amount of the corresponding reorganization energy. Interestingly, all measured luminescence decays are non-mono exponential with lifetime values in the microsecond range (Table 2). These observations are consistent with the typical mixed ^3LC - $^3\text{MLCT}$ emission originating from the $\text{Ir}(\text{ppy})_2$ moiety.

Table 2. Emission parameters

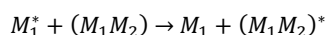
	rt ^a			77 K ^b	
	λ_{max} , nm	ϕ	τ , ns	λ_{max} , nm	τ , μs
2	n.d.	- (-)	- (-)	490, 524	5.5, 16.0
4	n.d.	- (-)	- (-)	477, 512	7.5, 22.4
6	n.d.	- (-)	- (-)	478, 512	7.4, 22.5
3	606	0.6×10^{-3} (0.4×10^{-3})	37.4 (26.6)	553, 608	8.0, 15.1
5	606	5.0×10^{-3} (3.2×10^{-3})	43.3 (27.3)	518, 568	6.9, 16.4
7	606	5.2×10^{-3} (3.0×10^{-3})	43.6 (27.3)	520, 568	6.5, 16.4

^a In de-aerated (air-equilibrated) CH_3OH solution at rt. ^b In $\text{MeOH}:\text{EtOH}$ (1:4) mixture at 77 K. $\lambda_{\text{exc}} = 390$ nm for steady-state and $\lambda_{\text{exc}} = 370$ nm for time-resolved measurements. n.d. is not detected.

A closer inspection of the overall spectral profiles reveals the presence of a low intensity peak or a shoulder on the high-energy side of the emission spectra of the iridium derivatives **3**, **5** and **7**. Further, the ratio between intensity of the low and high energy peaks increase at increasing concentration of the complex (see Figure 2 ESI, complex **7**) and it also depend on the excitation wavelength (see Figure 3 ESI). This is consistent with an excimer emission, as it is commonly observed in planar aromatic compounds where strong π -stacking interactions between pairing molecules are present, even in solution. In these cases, broad, structureless, and long-lived emissions with large Stokes shifts are commonly observed. These properties are typical of excimer features, as they indicate a very large displacement of the excited state relative to the geometry of the ground state. These bimolecular excited states can be formed by the direct optical excitation of the dimers already formed in the ground state (M_1M_2):



or by their excitation as a result of the energy transfer from mono-molecular triplet states:



In the latter case, a rise time in the luminescence decay of the excited dimeric species should be observed, corresponding to the decay time of the monomer, as a consequence of the energy

transfer process. In the systems investigated here we never observed any negative lifetime component in the kinetic analysis of the decays. Thus, it can be concluded that the dimer is already formed in the ground state. This conclusion is also supported by the observation of excitation spectra with different shape when recorded at the wavelength corresponding to the two main emission peaks (Figure 4 ESI).

In order to disentangle the contribution of the different components to the observed global luminescence and to attribute the relevant lifetime to the single monomeric and dimeric species we applied the global analysis to the individual kinetic traces recorded in time-resolved luminescence experiments. The decay-associated spectra (DAS) obtained by plotting the amplitudes of the individual kinetic components as function of the wavelength represent the true spectra of the individual decay components. These should be identical to the spectra that would be obtained if the components were isolated and then measured individually. This is not to be confused with procedures in which time-resolved spectra are recorded at different delay times after the excitation pulse. In contrast to the former, the latter will in general still represent weighted mixtures of the spectra of all decay components. Selected examples of the DAS obtained with the global analysis are reported in Figure 6 and the detailed procedure is reported in the Experimental section.

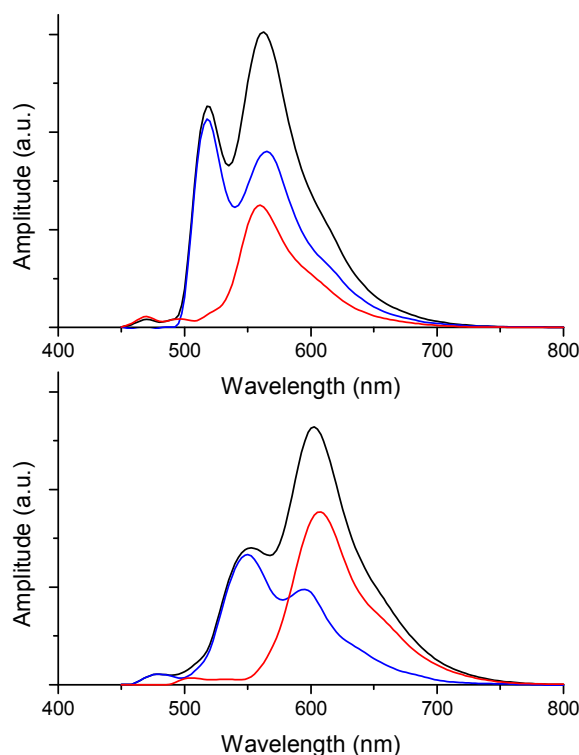


Figure 6. Decay Associated Spectra (DAS) of **3** (bottom) and **7** (top) in $\text{MeOH}:\text{EtOH}$ (1:4) at 77 K of monomer (blue line), dimer (red line) and sum of the two components (black line).

From the plot of single DAS it is evident the presence of two

species with different spectral shapes and lifetimes. In particular, a higher energy well structured emission with shorter lifetime can be attributed to the monomer (Figure 6, blue line), while the second longer-living component that displays a red-shifted almost unstructured spectrum is attributed to the emission from the dimer formed in the ground state (Figure 6, red line). Similar results have also been observed for the Rh derivatives **2** and **6** (Figure 6 ESI) and the discussion reported above about the behaviour of Ir complexes can be extended to the Rh derivatives as well.

It is interesting to note that all emission spectra recorded directly exciting powdered sample at 77 K display an unstructured and longer living luminescence, which is red-shifted with respect to the relevant emission in MeOH:EtOH frozen mixture (Figure 5 ESI). These might be safely attributed to excited states located on oligomeric species, where the excitons are delocalized over a longer distance with respect to the monomeric species. On the other end, there is no evidence of excimer formation from the emission spectra of Ir complexes in liquid solution at room temperature. This is a clear indication that the dimer formation can take place only in condensed media as a result of the solid state packing interactions.

Conclusions

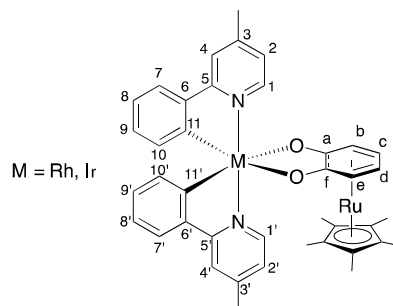
We have synthesized and fully characterized six Ir(III) and Rh(III) heteroleptic complexes with π -bonded dioxolene ligands. For two of them the x-ray molecular structures are reported, displaying solid-state packing between individual units with π - π interactions that generate 1D supramolecular chain. The photophysical properties of all complexes have been studied in solution at room temperature and in condensed media at low temperature. Notably, all our cyclometallated metal complexes containing π -bonded dioxolene ligands showed a bright emission in condensed media at 77 K, in contrast to that reported for coordination compounds with a non-metalated *o*-quinone ligand. The strong π - π interactions observed in the solid-state are retained also in solution allowing for the formation in the ground state of dimeric species. Emission from monomers and dimers has been observed and the contribution of the individual components has been resolved by means of analysis of the decay associated spectra (DAS). Finally, emissions from oligomeric species in the 1D supramolecular chain formed in the solid state have also been observed.

Experimental

General Information

All reactions were carried out under an argon atmosphere. Acetone was distilled from K_2CO_3 . CH_2Cl_2 was distilled from CaH_2 . Other reagents were obtained from commercial suppliers and used as received. Glassware was oven-dried prior to use. 1H NMR spectra were recorded at 300 MHz in CD_2Cl_2 and data are reported as follows: chemical shift in ppm from tetramethylsilane with the solvent as an internal indicator (CD_2Cl_2 δ 5.33 ppm), multiplicity (s = singlet, d = doublet, t = triplet, q = quartet, m = multiplet or overlap of non-equivalent resonances), integration. ^{13}C NMR spectra were recorded at 75.4 MHz in CD_2Cl_2 and data are reported as follows: chemical shift in ppm from

tetramethylsilane with the solvent as an internal indicator (CD_2Cl_2 δ 53.84 ppm), multiplicity with respect to proton (deduced from DEPT experiments). Infra-red (IR) spectra were measured using Tensor 27 (ATR diamond) Bruker spectrometer. IR data are reported as characteristic bands (cm^{-1}). Elemental analyses were performed by microanalytical service of ICSN at Gif-sur-Yvette on a Perkin Elmer 2400 apparatus.



[(mpcpy)₂Rh(1)](2)

This complex was prepared in two steps: The first step involves the *in-situ* preparation of the π -bonded ruthenium compound $[Cp^*Ru(o-C_6H_4O_2)][Cs]$ (**1-Cs**). Thus to a solution of $[Cp^*Ru(\eta^6\text{-catechol})][OTf]$ (100 mg, 0.20 mmol) in 5 mL of acetone was added Cs_2CO_3 (130 mg, 0.40 mmol) and the mixture was left for two hours of stirring. Then in a second step $AgOTf$ (51.4 mg, 0.20 mmol), in 5 mL of acetone is added to a solution of $[(mpcpy)_2Rh(\mu-Cl)]_2$ (113 mg, 0.10 mmol) in 5 mL of acetone. The resulting $AgCl$ formed is filtered off through a Celite plug. To this filtrate was added the solution of $[Cp^*M(o-C_6H_4O_2)][Cs]$ (**1-Cs**) formed *in-situ* and the resulting mixture is allowed to stir during one hour. The solvent was removed under vacuum and the residue is extracted by 20 mL of dichloromethane and filtered through neutral alumina. The resulting filtrate is then dried under vacuum to give the binuclear coordination assembly $[(mpcpy)_2Rh(1)](2)$ was isolated as a yellow-brown solid in 95% yield (166 mg, 0.19 mmol).
 Anal. Cald. For $C_{42}H_{41}N_2O_6RhRu.2H_2O$: C, 55.45; H, 4.99. Found: C, 55.54; H, 4.77.
 NMR 1H (400 MHz, CD_2Cl_2): 1.70 (15H, s, CH_3 -Cp*); 3.97 (3H, s, OCH_3); 4.05 (3H, s, OCH_3); 4.42 (1H, td, $J=5.5$, 1.2 Hz, Hc); 4.46 (1H, td, $J=5.5$, 1.2 Hz, Hd); 4.83 (1H, dd, $J=5.5$, 1.2 Hz, He); 4.94 (1H, dd, $J=5.5$, 1.2 Hz, Hb); 6.00 (1H, d, $J=7.8$ Hz, H10'); 6.19 (1H, d, $J=7.8$ Hz, H10); 6.75 (1H, td, $J=7.8$, 1.2 Hz, H9'); 6.78 (1H, td, $J=7.8$, 1.2 Hz, H9); 6.91 (1H, td, $J=7.8$, 1.2 Hz, H8'); 6.96 (1H, td, $J=7.8$, 1.2 Hz, H8); 7.64 (1H, dd, $J=5.9$, 1.6 Hz, H2'); 7.68 (1H, dd, $J=7.8$, 1.2 Hz, H7'); 7.75 (1H, dd, $J=7.78$, 1.2 Hz, H7); 7.90 (1H, dd, $J=5.9$, 1.6 Hz, H2); 8.34 (1H, d, $J=1.6$ Hz, H4'); 8.44 (1H, d, $J=1.6$ Hz, H4); 8.86 (1H, d, $J=5.9$ Hz, H1'); 9.27 (1H, d, $J=5.9$ Hz, H1).
 NMR ^{13}C (100 MHz, CD_2Cl_2): 10.0 (CH_3 -Cp*); 52.4 (OCH_3); 52.6 (OCH_3); 75.2 (Ce); 76.4 (Cd); 76.2 (Cc); 78.2 (Cb); 88.3 (Cq-Cp*); 117.7 (C4,4'); 120.3 (C2'); 120.4 (C2); 121.5 (C8,8'); 123.7 (C7); 123.8 (C7'); 128.6 (C9'); 128.8 (C9); 132.5 (C10'); 133.3 (C10); 137.4 (C3'); 137.5 (C3); 141.6 (Ca); 143.1 (C6); 143.3 (C6'); 147.6 (Cf); 149.5 (C1'); 150.8 (C1); 164.8 (CO'); 164.9 (CO); 165.5 (C5'); 165.7 (C5); 167.7 (C11); 167.9 (C11').
 IR (ATR, cm^{-1}): 3051; 2953; 2906; 2849; 1728; 1612; 1580; 1544; 1473; 1432; 1405; 1377; 1301; 1272; 1158; 1113;

1061 ; 1028 ; 968 ; 901 ; 848 ; 764 ; 730 ; 696 ; 662 ; 635 ; 591 ; 534 ; 454 ; 413 ; 348 ; 309 ; 272 ; 230.

[(mpepy)₂Ir(1)] (3)

The binuclear coordination assembly **3** was prepared in a similar way to that of **2**. Thus π -bonded ruthenium compound [Cp**Ru*(*o*-C₆H₄O₂)] [Cs] (**1-Cs**) (0.2 mmol) prepared *in situ*. Then a solution of AgOTf (51.4 mg, 0.20 mmol), in 5 mL of acetone is added to a solution of [(mpepy)₂Ir(μ -Cl)]₂ (131 mg, 0.10 mmol) in 5 mL of acetone the resulting AgCl formed in is filtered off on a Celite plug. To this filtrate was added the solution of [Cp**M*(*o*-C₆H₄O₂)] [Cs] (**1-Cs**) formed *in-situ* and the resulting mixture is allowed to stir during one hour. The solvent was removed under vacuum and the residue was extracted by 20 mL of dichloromethane, filtered through neutral alumina. The resulting filtrate is then dried under vacuum to give [(mpepy)₂Ir (**1**)] as a dark-purple solid in 99% yield (166 mg, 0.20 mmol).

Anal. Cald. For C₄₂H₄₁N₂O₆IrRu.2H₂O: C, 50.49; H, 4.54. Found: C, 50.50; H, 4.20.

NMR ¹H (400 MHz, CD₂Cl₂): 1.69 (15H, s, CH₃-Cp*); 3.97 (3H, s, OCH₃); 4.05 (3H, s, OCH₃); 4.42 (1H, m, Hc); 4.47 (1H, m, Hd); 4.88 (1H, dd, *J* = 5.5, 1.2 Hz, He); 4.97 (1H, dd, *J* = 5.5, 1.2 Hz, Hb); 6.02 (1H, dd, *J* = 7.8, 1.2 Hz, H10'); 6.21 (1H, dd, *J* = 7.8, 1.2 Hz, H10); 6.67 (1H, td, *J* = 7.8, 1.2 Hz, H9'); 6.69 (1H, td, *J* = 7.8, 1.2 Hz, H9); 6.82 (1H, td, *J* = 7.8, 1.2 Hz, H8'); 6.88 (1H, td, *J* = 7.8, 1.2 Hz, H8); 7.56 (1H, dd, *J* = 5.9, 1.7 Hz, H2'); 7.64 (1H, dd, *J* = 7.8, 1.2 Hz, H7'); 7.72 (1H, dd, *J* = 7.8, 1.2 Hz, H7); 7.81 (1H, dd, *J* = 5.9, 1.7 Hz, H2); 8.33 (1H, d, *J* = 1.7 Hz, H4'); 8.45 (1H, d, *J* = 1.7 Hz, H4); 8.90 (1H, d, *J* = 5.9 Hz, H1'); 9.26 (1H, d, *J* = 5.9 Hz, H1).
NMR ¹³C (100 MHz, CD₂Cl₂): 9.9 (CH₃-Cp*); 52.4 (OCH₃); 52.5 (OCH₃); 76.0 (Ce); 76.4 (Cd); 76.6 (Cc); 78.8 (Cb); 88.9 (Cq-Cp*); 117.3 (C4'); 117.4 (C4); 120.1 (C8'); 120.2 (C8); 120.3 (C2'); 120.9 (C2); 124.1 (C7); 124.3 (C7'); 128.8 (C9'); 129.1 (C9); 131.3 (C10'); 132.4 (C10); 136.8 (C3); 136.9 (C3'); 141.6 (Ca); 143.5 (C6,6'); 147.7 (C11); 147.9 (Cf); 148.2 (C1'); 148.5 (C11'); 149.5 (C1); 164.7 (CO'); 164.8 (CO); 168.8 (C5'); 168.9 (C5).
IR (ATR, cm⁻¹): 3634 ; 3046 ; 2952 ; 2907 ; 2849 ; 1724 ; 1611 ; 1580 ; 1536 ; 1473 ; 1461 ; 1432 ; 1406 ; 1377 ; 1347 ; 1318 ; 1298 ; 1270 ; 1224 ; 1157 ; 1111 ; 1058 ; 1026 ; 968 ; 900 ; 847 ; 765 ; 725 ; 695 ; 664 ; 628 ; 594 ; 536 ; 474 ; 451 ; 411 ; 344 ; 310 ; 262.

[(TBApepy)₂Rh (1)] (4)

In a flask containing [(mpepy)₂Rh (**1**)] (**2**) (43.7 mg, 0.05 mmol) was added TBAOH (0.8M in MeOH, 138 μ L, 0.11 mmol) in solution of 3 mL of EtOH/H₂O mixture (9/1). The mixture is allowed to stir overnight. After drying under vacuum, compound **4** is obtained as a yellow-brown solid in 97 % yield (50.8 mg, 48.7 μ mol).

Anal. Cald. For C₇₂H₁₀₅N₄O₆RhRu.6EtOH: C, 62.94 ; H, 8.87 ; N, 3.50 Found: C, 62.69 ; H, 8.97 ; 3.84.

NMR ¹H (400 MHz, CD₂Cl₂, signaux TBA omis): 1.71 (15H, CH₃-Cp*); 4.41 (2H, m, Hc,d); 4.77 (1H, m, He); 4.89 (1H, m, Hb); 6.02 (1H, d, *J* = 7.7 Hz, H10'); 6.19 (1H, d, *J* = 7.7 Hz, H10); 6.68 (2H, m, H9,9'); 6.81 (2H, m, H8,8'); 7.65 (3H, m, H2',7,7'); 7.93 (1H, m, H2); 8.32 (1H, d, *J* = 1.2 Hz, H4'); 8.44 (1H, d, *J* = 1.2 Hz, H4); 8.61 (1H, d, *J* = 5.8 Hz, H1'); 9.02

(1H, d, *J* = 5.7 Hz, H1).

NMR ¹³C (100 MHz, CD₃OD): 10.7 (CH₃-Cp*); 77.0 (Ce); 78.6 (Cd); 78.9 (Cc); 79.4 (Cb); 90.9 (Cq-Cp*); 119.1 (C4'); 119.2 (C4); 122.2 (C2'); 122.7 (C2); 122.8 (C8'); 122.9 (C8); 124.5 (C7); 124.7 (C7'); 129.4 (C9'); 129.6 (C9); 134.5 (C10'); 135.2 (C10); 140.3 (Ca); 145.1 (Cf); 145.8 (C6); 146.0 (C6'); 148.0 (C3'); 148.1 (C3); 150.0 (C1'); 151.4 (C1); 166.7 (C5'); 166.8 (C5); 167.6 (C11); 168.0 (C11'); 171.9 (CO); 172.0 (CO').

IR (ATR, cm⁻¹): 3051 ; 2963 ; 2931 ; 2871 ; 1607 ; 1578 ; 1538 ; 1475 ; 1403 ; 1343 ; 1301 ; 1254 ; 1153 ; 1102 ; 1059 ; 1028 ; 870 ; 786 ; 769 ; 734 ; 695 ; 660 ; 635 ; 591 ; 527 ; 458 ; 427 ; 344 ; 306 ; 282 ; 245.

[(TBApepy)₂Ir (1)] (5)

This compound was prepared in a similar fashion to that of **4**. [(TBApepy)₂Ir (**1**)] (**5**) is obtained as a red-brown solid in 89 % yield (63.1 mg, 44.5 μ mol).

Anal. Cald. For C₇₂H₁₀₅IrN₄O₆Ru.3Et₂O: C, 61.58; H, 8.31; N, 3.42. Found: C, 61.72; H, 8.61; N, 3.83.

NMR ¹H (400 MHz, CD₂Cl₂, signaux TBA omis): 1.70 (15H, s, CH₃-Cp*); 4.40 (2H, m, Hc,d); 4.80 (1H, m, He); 4.91 (1H, m, Hb); 6.04 (1H, d, *J* = 8.1 Hz, H10'); 6.22 (1H, d, *J* = 7.6 Hz, H10); 6.56 (2H, m, H9,9'); 6.73 (2H, m, H8,8'); 7.56 (3H, m, H2',7,7'); 7.87 (1H, m, H2); 8.30 (1H, d, *J* = 1.2 Hz, H4'); 8.43 (1H, d, *J* = 1.2 Hz, H4); 8.64 (1H, d, *J* = 5.9 Hz, H1'); 9.00 (1H, d, *J* = 5.9 Hz, H1).

NMR ¹³C (100 MHz, CD₃OD): 10.7 (CH₃-Cp*); 77.0 (Ce); 78.6 (Cd); 78.9 (Cc); 79.4 (Cb); 90.9 (Cq-Cp*); 119.1 (C4'); 119.2 (C4); 122.2 (C2'); 122.7 (C2); 122.8 (C8'); 122.9 (C8); 124.5 (C7); 124.7 (C7'); 129.4 (C9'); 129.6 (C9); 134.5 (C10'); 135.2 (C10); 140.3 (Ca); 145.1 (Cf); 145.8 (C6); 146.0 (C6'); 148.0 (C3'); 148.1 (C3); 150.0 (C1'); 151.4 (C1); 166.7 (C5'); 166.8 (C5); 167.6 (C11); 168.0 (C11'); 171.9 (CO); 172.0 (CO').

IR (ATR, cm⁻¹): 3050 ; 2962 ; 2930 ; 2871 ; 1609 ; 1577 ; 1533 ; 1473 ; 1380 ; 1343 ; 1225 ; 1153 ; 1110 ; 1059 ; 1028 ; 866 ; 787 ; 770 ; 733 ; 694 ; 664 ; 636 ; 595 ; 531 ; 474 ; 425 ; 347 ; 306 ; 270 ; 241.

[(Lipcpy)₂Rh (1)] (6)

In a Schlenk tube containing [(mpepy)₂Rh(**1**)] (43.7 mg, 0.05 mmol) was added LiOH (7.30 mg, 0.30 mmol) in 3 mL of EtOH/H₂O mixture (9/1). This mixture is allowed to stir overnight. After drying under vacuum, [(Lipcpy)₂Rh (**1**)] (**6**) is obtained as a yellow-green solid in 95 % (40.9 mg, 47.7 μ mol).

Anal. Cald. For C₄₀H₃₃Li₂N₂O₆RhRu.4LiOH.2EtOH: C, 50.65; H, 4.73; N, 2.68. Found: C, 50.75; H, 4.30; 2.35.

NMR ¹H (400 MHz, CD₃OD): 1.74 (15H, s, CH₃-Cp*); 4.63 (2H, m, Hc,d); 4.89 (1H, m, He); 4.98 (1H, m, Hb); 6.02 (1H, d, *J* = 7.8 Hz, H10'); 6.19 (1H, d, *J* = 7.8 Hz, H10); 6.67 (1H, m, H9'); 6.71 (1H, m, H9); 6.85 (1H, t, *J* = 7.4 Hz, H8'); 6.89 (1H, t, *J* = 7.4 Hz, H8); 7.54 (1H, dd, *J* = 7.9, 1.6 Hz, H2'); 7.67 (1H, d, *J* = 7.4 Hz, H7'); 7.74 (1H, d, *J* = 7.4 Hz, H7); 7.91 (1H, dd, *J* = 7.9, 1.6 Hz, H2); 8.36 (1H, brs, H4'); 8.49 (1H, brs, H4); 8.62 (1H, d, *J* = 5.9 Hz, H1'); 9.11 (1H, d, *J* = 5.9 Hz, H1).

NMR ¹³C (100 MHz, CD₃OD): 10.7 (CH₃-Cp*); 77.0 (Ce); 78.6 (Cd); 78.9 (Cc); 79.4 (Cb); 90.9 (Cq-Cp*); 119.1 (C4'); 119.2 (C4); 122.2 (C2'); 122.7 (C2); 122.8 (C8'); 122.9 (C8); 124.5

(C7) ; 124.7 (C7') ; 129.4 (C9') ; 129.6 (C9) ; 134.5 (C10') ; 135.2 (C10) ; 140.3 (Ca) ; 145.1 (Cf) ; 145.8 (C6) ; 146.0 (C6') ; 148.0 (C3') ; 148.1 (C3) ; 150.0 (C1') ; 151.4 (C1) ; 166.7 (C5') ; 166.8 (C5) ; 167.6 (C11) ; 168.0 (C11') ; 171.9 (CO) ; 172.0 (CO').

IR (ATR, cm⁻¹): 3049 ; 2972 ; 2906 ; 1604 ; 1580 ; 1539 ; 1472 ; 1411 ; 1379 ; 1296 ; 1228 ; 1161 ; 1093 ; 1052 ; 1026 ; 869 ; 771 ; 732 ; 698 ; 661 ; 635 ; 594 ; 537 ; 454 ; 343 ; 231 ; 222.

[(Lipcpy)₂Ir (I)] (7)

Dinuclear assembly **7** was prepared in a similar way to that of **6**. [(Lipcpy)₂Ir (I)] (**7**) is obtained as a red solid in 82% yield. (38.7 mg, 41.0 μmol.)

Anal. Calcd. For C₄₀H₃₃IrLi₂N₂O₆Ru.5LiOH.EtOH: C, 45.42; H, 3.99; N, 2.58. Found: C, 45.72; H, 3.70; N, 1.89

NMR ¹H (400 MHz, CD₃OD): 1.74 (15H, s, CH₃-Cp*) ; 4.64 (2H, m, Hc,d) ; 4.93 (1H, m, He) ; 5.00 (1H, m, Hb) ; 6.02 (1H, d, *J* = 7.4 Hz, H10') ; 6.18 (1H, d, *J* = 7.4 Hz, H10) ; 6.58 (1H, td, *J* = 7.4, 1.2 Hz, H9') ; 6.60 (1H, td, *J* = 7.4, 1.2 Hz, H9) ; 6.75 (1H, td, *J* = 7.4, 1.2 Hz, H8') ; 6.80 (1H, td, *J* = 7.4, 1.2 Hz, H8) ; 7.50 (1H, dd, *J* = 5.9, 1.6 Hz, H2') ; 7.62 (1H, d, *J* = 7.4 Hz, H7') ; 7.69 (1H, d, *J* = 7.4 Hz, H7) ; 7.85 (1H, dd, *J* = 5.9, 1.6 Hz, H2) ; 8.35 (1H, d, *J* = 1.6 Hz, H4') ; 8.49 (1H, d, *J* = 1.6 Hz, H4) ; 8.65 (1H, d, *J* = 5.9 Hz, H1') ; 9.09 (1H, d, *J* = 5.9 Hz, H1). NMR ¹³C (100 MHz, CD₃OD): 10.6 (CH₃-Cp*) ; 77.6 (Ce) ; 78.9 (Cd) ; 79.2 (Cc) ; 80.0 (Cb) ; 91.4 (Cq-Cp*) ; 118.8 (C4') ; 118.9 (C4) ; 121.4 (C8') ; 121.5 (C8) ; 122.0 (C2') ; 122.9 (C2) ; 124.8 (C7) ; 125.0 (C7') ; 129.6 (C9') ; 129.8 (C9) ; 133.4 (C10') ; 134.3 (C10) ; 140.6 (Ca) ; 145.7 (Cf) ; 146.4 (C6,6') ; 146.8 (C11) ; 147.5 (C3,3',11) ; 149.1 (C1') ; 150.4 (C1) ; 170.0 (C5') ; 170.1 (C5) ; 171.9 (CO) ; 172.0 (CO').

IR (ATR, cm⁻¹): 3045 ; 2904 ; 2824 ; 1603 ; 1581 ; 1533 ; 1464 ; 1412 ; 1379 ; 1291 ; 1227 ; 1158 ; 1127 ; 1062 ; 1027 ; 910 ; 865 ; 772 ; 732 ; 697 ; 664 ; 632 ; 595 ; 535 ; 491 ; 443 ; 342 ; 251.

Molecular structure determination of complexes **2** and **3**

A single crystal of each compound was selected, mounted onto a cryoloop, and transferred in a cold nitrogen gas stream. Intensity data were collected with a BRUKER Kappa-APExII diffractometer with graphite-monochromated Mo-Kα radiation (λ = 0.71073 Å). Data collection was performed with APEX2 suite (BRUKER). Unit-cell parameters refinement, integration and data reduction were carried out with SAINT program (BRUKER). SADABS (BRUKER) was used for scaling and multi-scan absorption corrections. In the WinGX suite of programs, the structure were solved with Sir92²⁷ or Superflip program²⁸ and refined by full-matrix least-squares methods using SHELXL-97.²⁹

Crystal data for **2** orange block-like crystals: C₄₂H₄₁N₂O₇RhRu, triclinic, *P*-1, *a* = 10.8039(4), *b* = 13.3968(4), *c* = 15.0329(2) Å, α = 100.649(2), β = 107.248(2), γ = 111.484(1)°, *V* = 1825.2(1) Å³, *Z* = 2, *T* = 200(2) K, ρ_{calc} = 0.921 mm⁻³, 45404 reflections measured, 10617 independent (*R*_{int} = 0.0192), 8558 observed [*I* ≥ 2σ(*I*)], 494 parameters, final *R* indices *R*₁ [*I* ≥ 2σ(*I*)] = 0.0343 and *wR*₂ (all data) = 0.0958, GOF on *F*² = 1.049, max/min residual electron density = 1.69/-0.92 e.Å⁻³.

All non-hydrogen atoms were refined anisotropically in **2**. H atoms were placed at calculated positions except those of O1w

water molecule.

Crystal data for **3**: C₄₂H₄₅IrN₂O₉Ru, monoclinic, *C* 2/*c*, *a* = 22.2991(14), *b* = 24.5147(15), *c* = 18.4529(12) Å, β = 122.944(3)°, *V* = 1825.2(1) Å³. *Z* = 8, *T* = 200(2) K, ρ_{calc} = 3.552 mm⁻³, 44781 reflections measured, 7451 independent (*R*_{int} = 0.0268), 5257 observed [*I* ≥ 2σ(*I*)], 483 parameters, final *R* indices *R*₁ [*I* ≥ 2σ(*I*)] = 0.0581 and *wR*₂ (all data) = 0.1884, GOF on *F*² = 1.095, max/min residual electron density = 2.39/-0.97 e.Å⁻³.

Atoms of the organometallic moiety were refined anisotropically. H atoms were placed at calculated positions. DIAMOND³⁰ was used to create graphical illustrations.

CCDC 974512, 974513, contain the supplementary crystallographic data for this paper. These data can be obtained free of charge from The Cambridge Crystallographic Data Centre via www.ccdc.cam.ac.uk/data_request/cif.

Photophysics

Absorption spectra of dilute CH₃OH solutions (*c* = 2 × 10⁻⁵ M) at rt were obtained using Perkin-Elmer Lambda 950 UV/Vis/NIR spectrophotometer. Steady-state photoluminescence spectra were measured in air-equilibrated and de-aerated solutions at rt, using an Edinburgh FLS920 fluorimeter, equipped with a Peltier-cooled R928P (200-850 nm) Hamamatsu PMT. Luminescence measurements at 77 K of MeOH:EtOH (1:4) mixtures were performed by employing quartz capillary tubes immersed in liquid nitrogen, and hosted within homemade quartz cold finger dewar. Luminescence quantum yields (*φ*) at rt were evaluated by comparing wavelength integrated intensities (*I*) of the corrected emission spectra with reference [Ru(bpy)₃]Cl₂ (*φ*_r = 0.028 in air-equilibrated water),²⁸ by using the following equation:

$$\phi = \phi_r \frac{(I n^2 / A)}{(I_r n_r^2 / A_r)}$$

where *A* and *A_r* are the absorbance values at the employed excitation wavelength, and *n* and *n_r* are the refractive indexes of the solvents, respectively for the investigated and the reference compound. The concentration was adjusted to obtain absorbance values *A* ≤ 0.1 at the excitation wavelengths. Band maxima and relative luminescence intensities are obtained with uncertainties of 2 nm and 10%, respectively.

Luminescence lifetimes were obtained using a Jobin-Yvon IBH 5000F TCSPC apparatus equipped with a TBX Picosecond Photon Detection Module and NanoLED/SpectraLED pulsed excitation sources. Analysis of luminescence decay profiles against time was accomplished using the Decay Analysis Software DAS6 provided by the manufacturer. The lifetime values were obtained with an estimated uncertainty of 10%.

Decay associated spectra (DAS) were obtained by global analysis of the kinetic data by using the global fitting module of the decay absorption spectra (DAS) 6.5 software (HORIBA Jobin Yvon) on the basis of a multi-exponential model:

$$F(\lambda, t) = \sum_i A_i(\lambda) \exp(t/\tau_i)$$

The goodness of the multi-component fitting was evaluated by the global χ² parameter and weighted residuals. The wavelength dependences of the amplitudes of the individual kinetic components were plotted as decay associated spectra.

Acknowledgements

We thank CNRS, UPMC, French ANR grant (project OPTOELECTR-OM ANR-11-BS07-001-01), the Italian CNR PM.P04.010 “Materiali Avanzati per la Conversione di Energia Luminosa” (MACOL) and the ESF-EUROCORES 10-5 EuroSolarFuels-FP-006 “Modular design of a bioinspired tandem cell for direct solar-to-fuel conversion” projects for supporting this work.

Notes and references

[†]Sorbonne Universités, UPMC Univ Paris 06, Université Pierre et Marie Curie, Institut Parisien de Chimie Moléculaire (IPCM) UMR 8232, 4 place Jussieu, 75252 Paris cedex 05, France. [‡]CNRS, Centre National de la Recherche Scientifique, Institut Parisien de Chimie Moléculaire (IPCM) UMR 8232, 4 place Jussieu, 75252 Paris cedex 05, France. Fax: (33)1-44-27-38-41 E-mail: hani.amouri@upmc.fr

[§]Institut de Recherche de Chimie Paris, CNRS – Chimie ParisTech, 11 rue Pierre et Marie Curie, 75005 Paris, France.

[‡]Istituto per la Sintesi Organica e la Fotoreattività (ISOF), Consiglio Nazionale delle Ricerche (CNR), Via Gobetti 101, 40129 Bologna, Italy. E-mail: andrea.barbieri@isof.cnr.it

[†] Electronic Supplementary Information (ESI) available: additional results of the photophysical investigation. See DOI: 10.1039/b000000x/

1. D. N. Hendrickson and C. G. Pierpont, *Top. Curr. Chem.*, 2004, **234**, 63-95.
2. A. B. P. Lever, *Coord. Chem. Rev.*, 2010, **254**, 1397-1405.
3. M. D. Ward and J. A. McCleverty, *J. Chem. Soc.-Dalton Trans.*, 2002, 275-288.
4. (a) W. Kaim and B. Sarkar, *Coord. Chem. Rev.*, 2007, **251**, 584-594; (b) J. L. Boyer, J. Rochford, M. K. Tsai, J. T. Muckerman and E. Fujita, *Coord. Chem. Rev.*, 2010, **254**, 309-330.
5. (a) R. S. da Silva, S. I. Gorelsky, E. S. Dodsworth, E. Tfouni and A. B. P. Lever, *J. Chem. Soc.-Dalton Trans.*, 2000, 4078-4088; (b) H. Masui, A. L. Freda, M. C. Zerner and A. B. P. Lever, *Inorg. Chem.*, 2000, **39**, 141-152.
6. R. J. Mortimer, *Chem. Soc. Rev.*, 1997, **26**, 147-156.
7. F. Hartl, P. Rosa, L. Ricard, P. Le Floch and S. Zalis, *Coord. Chem. Rev.*, 2007, **251**, 557-576.
8. M. K. Nazeeruddin, P. Pechy, T. Renouard, S. M. Zakeeruddin, R. Humphry-Baker, P. Comte, P. Liska, L. Cevey, E. Costa, V. Shklover, L. Spiccia, G. B. Deacon, C. A. Bignozzi and M. Gratzel, *J. Am. Chem. Soc.*, 2001, **123**, 1613-1624.
9. C. R. Rice, M. D. Ward, M. K. Nazeeruddin and M. Gratzel, *New J. Chem.*, 2000, **24**, 651-652.
10. R. Marczak, F. Werner, J. F. Gnichwitz, A. Hirsch, D. M. Guldi and W. Peukert, *J. Phys. Chem. C*, 2009, **113**, 4669-4678.
11. C. S. Grange, A. Meijer and M. D. Ward, *Dalton Trans.*, 2010, **39**, 200-211.
12. G. H. Spikes, E. Bill, T. Weyhermuller and K. Wieghardt, *Angew. Chem.-Int. Edit.*, 2008, **47**, 2973-2977.
13. A. B. P. Lever, H. Masui, R. A. Metcalfe, D. J. Stufkens, E. S. Dodsworth and P. R. Auburn, *Coord. Chem. Rev.*, 1993, **125**, 317-331.
14. (a) S. Bhattacharya and C. G. Pierpont, *Inorg. Chem.*, 1992, **31**, 35-39; (b) S. Bhattacharya, S. R. Boone, G. A. Fox and C. G. Pierpont, *J. Am. Chem. Soc.*, 1990, **112**, 1088-1096.
15. D. E. Wheeler and J. K. McCusker, *Inorg. Chem.*, 1998, **37**, 2296-2307.
16. S. G. Abuabara, C. W. Cady, J. B. Baxter, C. A. Schmuttenmaer, R. H. Crabtree, G. W. Brudvig and V. S. Batista, *J. Phys. Chem. C*, 2007, **111**, 11982-11990.
17. (a) F. Hartl and A. Vlcek, *Inorg. Chem.*, 1996, **35**, 1257-1265; (b) F. Hartl and A. Vlcek, *Inorg. Chem.*, 1992, **31**, 2869-2876.
18. (a) J. Moussa, M. N. Rager, L. M. Chamoreau, L. Ricard and H. Amouri, *Organometallics*, 2009, **28**, 397-404; (b) C. W. Lange, M. Foldeaki, V. I. Nevodchikov, V. K. Cherkasov, G. A. Abakumov and C. G. Pierpont, *J. Am. Chem. Soc.*, 1992, **114**, 4220-4222.
19. (a) B. Hirani, J. Li, P. I. Djurovich, M. Yousufuddin, J. Ongaard, P. Persson, S. R. Wilson, R. Bau, W. A. Goddard and M. E. Thompson, *Inorg. Chem.*, 2007, **46**, 3865-3875; (b) P. Barbaro, C. Bianchini, P. Frediani, A. Meli and F. Vizza, *Inorg. Chem.*, 1992, **31**, 1523-1529.
20. J. Best, I. V. Sazanovich, H. Adams, R. D. Bennett, E. S. Davies, A. Meijer, M. Towrie, S. A. Tikhomirov, O. V. Bouganov, M. D. Ward and J. A. Weinstein, *Inorg. Chem.*, 2010, **49**, 10041-10056.
21. (a) H. Amouri, R. Thouvenot, J. Vaissermann and M. Gruselle *Organometallics* 2001, **20**, 1904-1906; (b) H. Amouri, J. Vaissermann, Y. Besace, K. P. C. Vollhardt, G. E. Ball *Organometallics* 1993, **12**, 605-609; (c) H. Amouri, R. Thouvenot, M. Gruselle *C. R. Chimie*, 2002, **5**, 257-262; (d) D. Vichard, M. Gruselle, H. Amouri *J. Chem. Soc., Chem. Comm.* 1991, 46-48.; (e) D. Vichard, M. Gruselle, H. Amouri, J. Vaissermann *Organometallics* 1992, **11**, 976-979; (f) H. Amouri, R. Caspar, M. Gruselle, C. Guyard-Duhayon, K. Boubekeur, D. A. Lev, L. S. B. Collins, D. B. Grotjahn, *Organometallics* 2004, **23**, 4338-4341; (g) J. Le Bras, H. Amouri and J. Vaissermann, *J. Organomet. Chem.*, 1998, **553**, 483-485; (h) J. Le Bras, M. N. Rager, Y. Besace, H. Amouri and J. Vaissermann, *Organometallics*, 1997, **16**, 1765-1771; (i) J. Moussa, C. Guyard-Duhayon, P. Herson, H. Amouri, M. N. Rager and A. Jutand, *Organometallics*, 2004, **23**, 6231-6238.
22. (a) J. Moussa, D. A. Lev, K. Boubekeur, M. N. Rager and H. Amouri, *Angew. Chem.-Int. Edit.*, 2006, **45**, 3854-3858; (b) J. Moussa, M. N. Rager, K. Boubekeur and H. Amouri, *Eur. J. Inorg. Chem.*, 2007, 2648-2653.
23. (a) H. Amouri, J. Moussa, A. K. Renfrew, P. J. Dyson, M. N. Rager and L. M. Chamoreau, *Angew. Chem.-Int. Edit.*, 2010, **49**, 7530-7533. (b) J. Dubarle-Offner, C. M. Clavel, G. Gontard, P. J. Dyson, H. Amouri *Chem. Eur. J.* DOI: 10.1002/chem.201304991.
24. J. Moussa and H. Amouri, *Angew. Chem.-Int. Edit.*, 2008, **47**, 1372-1380.
25. J. Moussa, K. M. C. Wong, L. M. Chamoreau, H. Amouri and V. W. Yam, *Dalton Trans.*, 2007, 3526-3530.
26. A. Damas, B. Ventura, M. R. Axet, A. Degli Esposti, L.-M. Chamoreau, A. Barbieri and H. Amouri, *Inorg. Chem.*, 2010, **49**, 10762-10764.
27. (a) L. Flamigni, A. Barbieri, C. Sabatini, B. Ventura and F. Barigelletti, *Top. Curr. Chem.*, 2007, **281**, 143-203; (b) M. T. Indelli, C. Chiorboli and F. Scandola, *Top. Curr. Chem.*, 2007, **280**, 215-255.
28. M. Montalti, A. Credi, L. Prodi and M. T. Gandolfi, *Handbook of Photochemistry*, 3rd edn., CRC Press, Taylor & Francis, Boca Raton, 2006.
29. (a) G. Calogero, G. Giuffrida, S. Serroni, V. Ricevuto and S. Campagna, *Inorg. Chem.*, 1995, **34**, 541-545; (b) M. Polson, S. Fracasso, V. Bertolasi, M. Ravaglia and F. Scandola, *Inorg. Chem.*, 2004, **43**, 1950-1956.
30. (a) A. Damas, B. Ventura, J. Moussa, A. Degli Esposti, L. M. Chamoreau, A. Barbieri and H. Amouri, *Inorg. Chem.*, 2012, **51**, 1739-1750. (b) A. Damas, M. Pia Gullo, M. N. Rager, A. Jutand, A. Barbieri, H. Amouri *Chem. Comm.* 2013, **49**, 3796-3798.